






Research Article

CircRNA FAT1 Regulates Osteoblastic Differentiation of Periodontal Ligament Stem Cells via miR-4781-3p/SMAD5 Pathway

Yu Ye ^{1,2}, Yue Ke ^{1,2}, Liu Liu ^{1,2}, Tong Xiao ^{1,2}, and Jinhua Yu ^{1,2,3}

¹Jiangsu Key Laboratory of Oral Diseases, Nanjing Medical University & Department of Endodontic, Affiliated Hospital of Stomatology, Nanjing Medical University, Nanjing, China

²Institute of Stomatology, Nanjing Medical University, Nanjing, China

³Jiangsu Province Engineering Research Center of Stomatological Translational Medicine, Nanjing, China

Correspondence should be addressed to Jinhua Yu; yujinhua@njmu.edu.cn

Received 19 August 2021; Revised 19 November 2021; Accepted 4 December 2021; Published 29 December 2021

Academic Editor: Christian Morsczeck

Copyright © 2021 Yu Ye et al. This is an open access article distributed under the Creative Commons Attribution License, which permits unrestricted use, distribution, and reproduction in any medium, provided the original work is properly cited.

The ability of human periodontal ligament stem cells (PDLSCs) to differentiate into osteoblasts is significant in periodontal regeneration tissue engineering. In this study, we explored the role and mechanism of circRNA FAT1 (circFAT1) in the osteogenic differentiation of human PDLSCs. The proliferation capacity of PDLSCs was evaluated by EdU and CCK-8 assay. The abilities of circFAT1 and miR-4781-3p in regulating PDLSC differentiation were analyzed by western blot, reverse transcription-polymerase chain reaction (RT-PCR), alkaline phosphatase (ALP), and Alizarin red staining (ARS). A nucleocytoplasmic separation experiment was utilized for circFAT1 localization. A dual-luciferase reporter assay confirmed the binding relationship between miR-4781-3p and circFAT1. It was showed that circFAT1 does not affect the proliferation of PDLSCs. The osteogenic differentiation of PDLSCs was benefited from circFAT1, which serves as a miRNA sponge for miR-4781-3p targeting SMAD5. Both knockdown of circFAT1 and overexpression of miR-4781-3p suppressed the osteogenic differentiation of PDLSCs. Thus, circFAT1 might be considered as a potential target of PDLSCs mediated periodontal bone regeneration.

1. Introduction

Periodontitis is a chronic oral infectious disease characterized by the disruption of periodontal supporting tissues integrity, including the destruction of alveolar bone, periodontal ligament (PDL), and cementum [1]. As one of the most common infection-driven diseases, Periodontitis can affect 90% of the global population [2]. Periodontitis can lead to loss of periodontal attachment and, if left untreated, can eventually lead to early tooth loss [3]. At present, the biggest challenge in the treatment of periodontitis is periodontal regeneration. Human periodontal ligament stem cells (PDLSCs) are mesenchymal stem cells (MSCs) derived from tooth tissues with high osteogenesis potential. Therefore, studying the molecular mechanism of osteogenic differ-

entiation of PDLSCs is the keystone of the clinical application of tooth regeneration and osteogenic tissue engineering.

Noncoding RNA (ncRNA) is a kind of RNA transcribed from the genome, which can function at the RNA level rather than traditionally encode protein [4]. ncRNA can be classified into three types: (1) microRNA (miRNAs), siRNAs, and new noncoding small RNAs (piRNAs) with a length less than 50 NT; (2) the length ranges from 50 to 500 NT, including ribosomal RNA (rRNA) and transfer RNA (tRNA); and (3) longer than 500 NT, including long noncoding RNAs (lncRNAs) and circular RNAs (circRNAs) [4, 5]. miRNA is an endogenous noncoding small single-stranded RNA with a length of about 22 nucleotides [6]. It is worth noting that miRNAs participate in bone metabolism by acting on target genes related to osteogenic differentiation.

Many miRNAs have been proved to participate in the osteogenic differentiation of PDLSCs [7–9].

The TGF- β signaling pathway is an essential pathway for the osteogenic differentiation procession. It relies on multiple SMAD proteins, such as receptor-regulated SMAD (R-SMAD), common SMAD (co-SMAD), and inhibitory SMAD (I-SMAD) [10]. SMAD family member 5 (SMAD5) is a R-SMAD protein. As a transcription factor, it takes part in the osteogenic differentiation of BMSCs [11]. When osteogenic signals are transmitted to the cytoplasm of BMSCs, phosphorylated-SMAD5 is directed to the nucleus and then regulates the expression of osteogenesis-related target genes [10]. The nuclear translocation of SMAD5 is key to osteogenesis signal transduction. LncTUG1 may inhibit the osteogenic differentiation of bone marrow mesenchymal stem cells (BMSCs) by targeting SMAD5 [12]. miR-24-3p targets SMAD5 to promote the osteogenic potential of PDLSCs [13]. miR-21, miR-17-5p, and miR-106b-5p inhibit bone formation by targeting SMAD5 [14, 15]. In another study, miR-222-3p depressed osteogenic differentiation of BMSCs, revealing the regulation of the SMAD5-RUNX2 signal axis [11].

CircRNAs are characterized by a special structure of continuous covalent closed loop, which has higher conservation and stability [16, 17]. CircRNAs have been applied in clinical treatment or disease diagnosis as biomarkers or targets [18]. Evidence has been demonstrated that circRNAs played a key role in developing numerous diseases by regulating key steps such as gene transcription, translation, and splicing [19, 20]. Studies on the accumulation of circRNAs revealed their important role in bone metabolism-related diseases [21]. Recently, circRNAs are discovered to be involved in maintaining the pluripotency of human embryonic stem cells (ESCs) [22], self-renewal ability of intestinal stem cells [23], the differentiation potential of osteoblasts and osteoclasts [24, 25], and even the rat liver regeneration [26]. So far, circRNAs have been well known as miRNA sponges. Thus, circRNAs work as posttranscriptional regulators, sponging with miRNAs and producing important biological effects [27]. Accumulating evidence shows that circRNAs play a nonnegligible role in many diseases, including periodontitis. Acting as a miR-7 sponge to upregulate Krueppel-like factor 4 (KLF4) expression, circCDR1 promoted PDLSCs stemness [28]. circCDK8 inhibited the osteogenic differentiation of PDLSCs by triggering autophagy activation in a hypoxic microenvironment [29].

CircRNA FAT1 (circFAT1), as a relatively new circRNA, has been reported to increase cell stemness of cancer cells through upregulation of miR-21 [30]. In breast cancer, circFAT1 may regulate miR-525-5P/SKA1 resistance through Notch and Wnt pathways, providing a potential target for breast cancer treatment [31]. circFAT1 has not been reported in any published literature about its effect on the osteogenic differentiation of PDLSCs. In our previous study, it was found that the expression of circFAT1 decreased in the hypoxic microenvironment, while the osteogenic differentiation ability of PDLSCs decreased. Thus, it can be inferred that circFAT1 may be positively correlated with the osteogenic differentiation of PDLSCs. miR-4781-3p was

only found to be upregulated in Alzheimer's disease patients [32]. At present, there is no more literature report, and its exact role and mechanism in osteogenesis are still unclear. Sequencing results and preliminary experimental results showed that there is a binding relationship between circFAT1/miR-4781-3p/SMAD5, which may be involved in regulating the osteogenic differentiation of PDLSCs. Combined with bioinformatics predictions, this study investigates the mechanism by which circFAT1 may act as a sponge of miR-4781-3p to regulate SMAD5 and then affect the osteogenic differentiation of PDLSCs. It is expected to provide a new therapeutic target for exploring the periodontal regeneration mediated by PDLSCs.

2. Materials and Methods

2.1. Animals. Male SD rats (5 weeks old) were purchased from the experimental animal center of Nanjing Medical University and raised at the SPF level. All animal experiments were conducted according to the regulations of the ethics committee of Nanjing Medical University (IACUC-2010051). SD rats were anesthetized by intraperitoneal injection (1% sodium barbital) to establish a skull defect model. Make a 10 mm incision in the rat head and perform a trephine osteotomy on the cranial platform. Make two 5 mm diameter holes symmetrically on both sides of the midline of the skull. Implant the cell mass and the corresponding control group into the pores. Then, suture the wound. At week 8, skull tissue was collected for further analysis.

2.2. Microcomputed Tomography (micro-CT), Hematoxylin-Eosin (H&E), and Masson Staining. The rats were sacrificed eight weeks after surgery, and the cranial tissue was collected. The tissues were fixed with 4% paraformaldehyde (PFA) for one week and 75% ethanol for micro-CT evaluation. 3D images of the mineralized tissues were reconstructed using Sky scan software. The bone volume/tissue volume (BV/TV) of each sample was collected for analysis. After micro-CT evaluation, the tissues were demineralized in 14% EDTA solution for eight weeks, dehydrated by an automatic dehydrator, and embedded in paraffin. Paraffin sections were cut into tissue sections 5 mm thick for H&E and Masson staining.

2.3. Tissue Collection and Cell Culture. The premolars of healthy people extracted due to orthodontics were collected. Scrape the periodontal ligament tissue in the 1/3 area of the root, transfer it into a 10 cm sterile dish, and add α -minimum primary medium (α -MEM, GIBCO, California, USA) to keep the tissue moist, sharply separate about 1m³ tissue blocks of periodontal ligament tissue, lay the separated tissue blocks in culture flask at a spacing of 1 mm, inverted the flask, and add α -MEM (including 100 ml/L fetal bovine serum, 100u/ml penicillin, and 100 μ g/ml streptomycin). The culture flask was placed in an incubator at 37°C and 5% CO₂ for culture. Turn over the tissue after 4 hours. The solution was changed every three days. The cells grew up to 80% and were sub cultured when confluence. A monoclonal screening method was adopted to purify PDLSCs. 3-5

generations of PDLSCs were cultivated for the follow-up experiments. The Ethics Committee of Nanjing Medical University School approved the relevant experiments (NJMU-2018202).

2.4. Adipogenic Differentiation. PDLSCs in the logarithmic growth stage were inoculated into the culture dish following the cell density of 2×10^4 cells/cm². The cells were cultured at 37°C, 5% CO₂ environment to the confluence of 90-100%, the supernatant was discarded, and the adipogenic induction differentiation medium induction solution (Cyagen, Guangzhou, China) was added. After three days, the culture medium was replaced with an adipogenic differentiation medium induction solution. After one day of culture, it was replaced with adipogenic differentiation medium maintenance solution for three days. The cells were induced for 14-21 days according to the above liquid exchange frequency; then, the medium was aspirated. After washing once with $1 \times$ PBS, PDLSCs were fixed with 4% PFA solution at room temperature for 30-60 minutes, and oil red O staining was performed.

2.5. Chondrogenic Differentiation. Transfer 3×10^5 PDLSCs to a 15 ml centrifuge tube and centrifuge at 250 g for 4 minutes. Discard the supernatant, add 0.5 ml of chondrogenic differentiation medium basal solution, resuspend the cells, and centrifuge at 150 g for 5 minutes. Carefully discard the supernatant, add 0.5 ml chondrogenic differentiation medium induction solution (Cyagen, Guangzhou, China), resuspend the cells, and centrifuge at 150 g for 5 minutes. Unscrew the 15 ml centrifuge tube cap slightly and place it at 37°C, 5% CO₂ incubator. After 24 hours, observe the deformation and accumulation of the cell pellets. The cell mass was transferred to a 24-well plate. Replace with induction solution every two days. After 21 days, the cartilage balls were fixed and sliced for Alcian blue staining.

2.6. Plasmid and siRNA Transfection. PDLSCs were inoculated in medium dishes and transfected when the fusion rate reached 50-60%. The transfected siRNA and plasmid were constructed by the company (RiboBio, Guangzhou, China). miR-4781-3p mimics (mimics, 50 nM), mimic negative control (NC, 50 nM), miR-4781-3p inhibitor (inhibitor, 100 nM), and inhibitor negative control (iNC, 100 nM) were mixed with Ribofect™ CP Kit (RiboBio, Guangzhou, China). Cells were stimulated for 24-72 hours. Similarly, PDLSCs transfected with circFAT1, SMAD5 siRNA, and negative controls (si-FAT1, si-SMAD5, NC, 100 nM) were performed similar operations. Luciferase reporter plasmids of circFAT1 and miR-4781-3p were constructed by predicting the binding sites. Lipofectamine 2000 was used as a transfection agent to transfect HEK-293T cells.

2.7. Cell Proliferation Assay. Different stimuli were adopted to treat PDLSCs and then add 100 μl of cell suspension in a 96-well plate. Incubate the culture plate for 0, 1, 3, 5, and 7 days. Add 10 μl of CCK8 solution to each well and incubate the culture plate in the incubator for 1-4 hours. Measure the absorbance at 450 nm with a microplate reader. EdU was detected by Cell-Light™ EdU Apollo®567 *In Vitro* Imaging Kit (RiboBio, Guangzhou, China). The transfected

PDLSCs were seeded in glass slides. After labeling with EdU, fixing the cells, staining with Apollo, and staining DNA with Hoechst 33342, the cells were observed with a fluorescence microscope. ImageJ software was used to calculate cell DNA replication efficiency.

2.8. Flow Cytometry. After the cells were treated differently, they were digested with trypsin without EDTA (Beyotime, Shanghai, China) and collected. The cells were resuspended in PBS and centrifuged twice, then resuspended in 100 μL of PBS, and added with CD34, CD45, CD29, CD90, and CD105 surface molecule antibodies. After incubating on ice in the dark for 30 minutes, the cells were centrifuged with PBS. Then, the supernatant was removed, and flow cytometry analysis (BD Biosciences, CA, USA) was performed.

2.9. Quantitative Real-time RT-PCR (RT-qPCR). TRIzol (Invitrogen, CA, USA) method was applied to extract RNA from cells. Then, the RNA was reverse transcribed to cDNA by a reverse transcription kit. Design the corresponding primers. Use the CHAMQ Universal SYBR qPCR Master Mix (Vazyme, Nanjing, China) reagent to set up the related program on the ABI QuantStudio 7 fluorescence quantitative PCR instrument (Applied Biological System) according to the instructions. The primer list is shown in Table 1.

2.10. Western Blot Analysis. The cell lysate was used to lyse the cells, the supernatant was taken after centrifugation, and the protein loading buffer was added; then, the protein sample was boiled. Perform electrophoresis experiments with 10% SDS-PAGE gel at 70 V constant pressure and transfer membrane at 300 mA constant current. After sealing with 5% milk for 2 hours, add primary antibody diluent (anti-COL1A (Proteintech, USA), anti-COL3A (Proteintech, USA), anti-RUNX2 (ABCAM, UK), anti-OSX (ABCAM, UK), anti-SMAD5 (Proteintech, USA), and anti-GAPDH (Cell signaling Technology, USA)). After 4°C overnight, protein bands were obtained by chemiluminescence gel imaging system. Then, the grey value analysis was performed.

2.11. Alkaline Phosphatase (ALP) Activity Assay and Alizarin Red Staining (ARS). After seven days of induction of PDLSCs by adding mineralization induction solution, the ALP activity was detected, and ALP staining was performed. The alkaline phosphatase detection kit (Jiancheng, Nanjing, China) and the alkaline phosphatase color reagent kit (Beyotime, Shanghai, China) were used for detection. After 14 days of induction, 4% PFA was added to fix PDLSCs and then wash the cells with PBS 3 times. The cells were observed under the microscope after being incubated with Alizarin Red dye solution (40 mM, pH = 4.2, Sigma-Aldrich) for at least 1 hour. Cetylpyridine chloride (CPC, 100 mM) was used to dissolve calcified nodules, and the relative calcium mass was calculated according to the absorbance at 562 nm.

2.12. Immunofluorescence Staining. The treated PDLSCs were digested and placed on the cell slides. The next day, the culture medium was discarded and fixed with 4% PFA. Perforate the cells with Triton X-100 (Beyotime, Shanghai,

TABLE 1: Sense and antisense primers for RT-qPCR.

Genes	Primers	Sequences (5'-3')
GAPDH	Forward	TCACCAGGGCTGCCATCTGCTCTC
	Reverse	TTGCAGTGGCAAAGTGGAGATTGTTG
COL1A	Forward	TCTGACTGGAAGAGCGGAGAG
	Reverse	GAGTGGGGAACACACAGGTCT
COL3A	Forward	CTGTGAATCATGCCCTACTGGTC
	Reverse	AAGCCTCTGTGTCCTTTCATACC
RUNX2	Forward	TCTTAGAACAAATTCTGCCCTTT
	Reverse	TGCTTTGGTCTTGAAATCACA
OSX	Forward	GCCTACTTACCCGTCTGACTTT
	Reverse	GCCCACTATTGCCAACTGC
SMAD5	Forward	ACCGCACATGCCACAAAAC
	Reverse	CAGGGGAAGGAGGATAGGG
FAT1	Forward	GATGAGGACGCCAGAAGAGA
	Reverse	CAAATGTCTCCCCATTGCTT
miR-4781-3p	Forward	CGCGCGGGGAACCCGC
	Reverse	AGTGCAGGGTCCGAGGTATT

China) for 12 minutes. Then, the cells were treated with block goat serum for 2 hours at 37°C, washed with PBS 3 times. Then, incubate the cells overnight at 4°C with ALP antibody diluted at 1:100, and the liquid with fluorescent secondary antibody was changed at room temperature in the dark for 2 hours. Phalloidin (Yeasen, Shanghai, China) was added to the cells for 30 minutes. DAPI (Beyotime, Shanghai, China) was dyed for 90 seconds for nuclear staining. Then, it was observed under a fluorescence microscope (Leica, Germany).

2.13. Nucleocytoplasmic Separation. Isolate cytoplasmic cytonuclear RNA from cells according to the manufacturer's instructions. Cell precipitation was collected after being digested and washed. Add 400 μ L Cell Separation Buffer to the cell precipitation. After being incubated for 10 minutes, the mixture was centrifugated at 500 \times g for 1 minute to separate the cytoplasm and nucleus. Then, the nuclear residue was dissolved in a Cell Disruption Buffer. The nuclear and cytoplasmic samples were mixed thoroughly up with 2 \times Lysis/Binding Solution at RT. Anhydrous ethanol was added to each sample, and the mixture was centrifuged for 1 minute. Wash solutions 1 and 2/3 were utilized to wash the samples. RNA from cytoplasm and nucleus were separately added to the preheated eluent and then collected for RT-PCR analysis.

2.14. RNA Fluorescence In Situ Hybridization (FISH). PDLSCs were cultured on confocal plates. Then, after fixation with 4% PFA, the cells were washed with PBS and pre-cooled with 0.5% Triton X-100 for 5 minutes at 4°C. Each well was prehybridized with 500 μ L prehybridization buffer at 37°C for 30 minutes. The FISH probe mixture or internal reference probe was then added to the 200 μ L preheated hybridization buffer. PDLSCs were then incubated overnight in darkness at 37°C in a hybridization buffer containing

FISH probes. The cells were washed three times with the hybridized lotion at a concentration gradient of 42°C for 5 minutes, and DAPI has stained again in the dark for 10 minutes. Wash three times and use PBS to remove excess liquid. The cell photographs were taken with LSM 710 confocal microscope (Leica, Germany).

2.15. Dual-Luciferase Reporter Assay. miR-4781-3p and negative control were transfected into HEK-293 T cells. 100 ng circFAT1 or SMAD5 wild-type reporter plasmid and 20 ng renilla luciferase (RL) reporter plasmid was simultaneously transfected into HEK-293 T cells. Set circFAT1 or SMAD5 reported plasmid mutations as the control. After 48 hours, a dual-luciferase reporter gene detection kit (Promega, Madison, USA) was used to detect luciferase activity.

2.16. Statistical Analysis. Each experiment was repeated three times or more. Statistical analyzes were conducted with SPSS 17.0. *t*-test or one-way analysis of variance was used to the analyzed difference among groups. $P < 0.05$ was considered statistically different.

3. Results

3.1. Identification of PDLSCs and Verification of PDLSCs Multidirectional Differentiation Ability

- (1) Primary PDLSCs crawled out from around the tissue, mostly long spindle-shaped and growing densely (Figure 1(a)). After screening the cells cultured by the monoclonal method, multiple scattered cell colonies similar to clones could be seen (Figures 1(a)–1(c)). Flow cytometry results showed that CD29, CD73, CD90, and CD105 were positive in PDLSCs. In addition, both CD45 and CD34 were negative (Figure 1(b)).

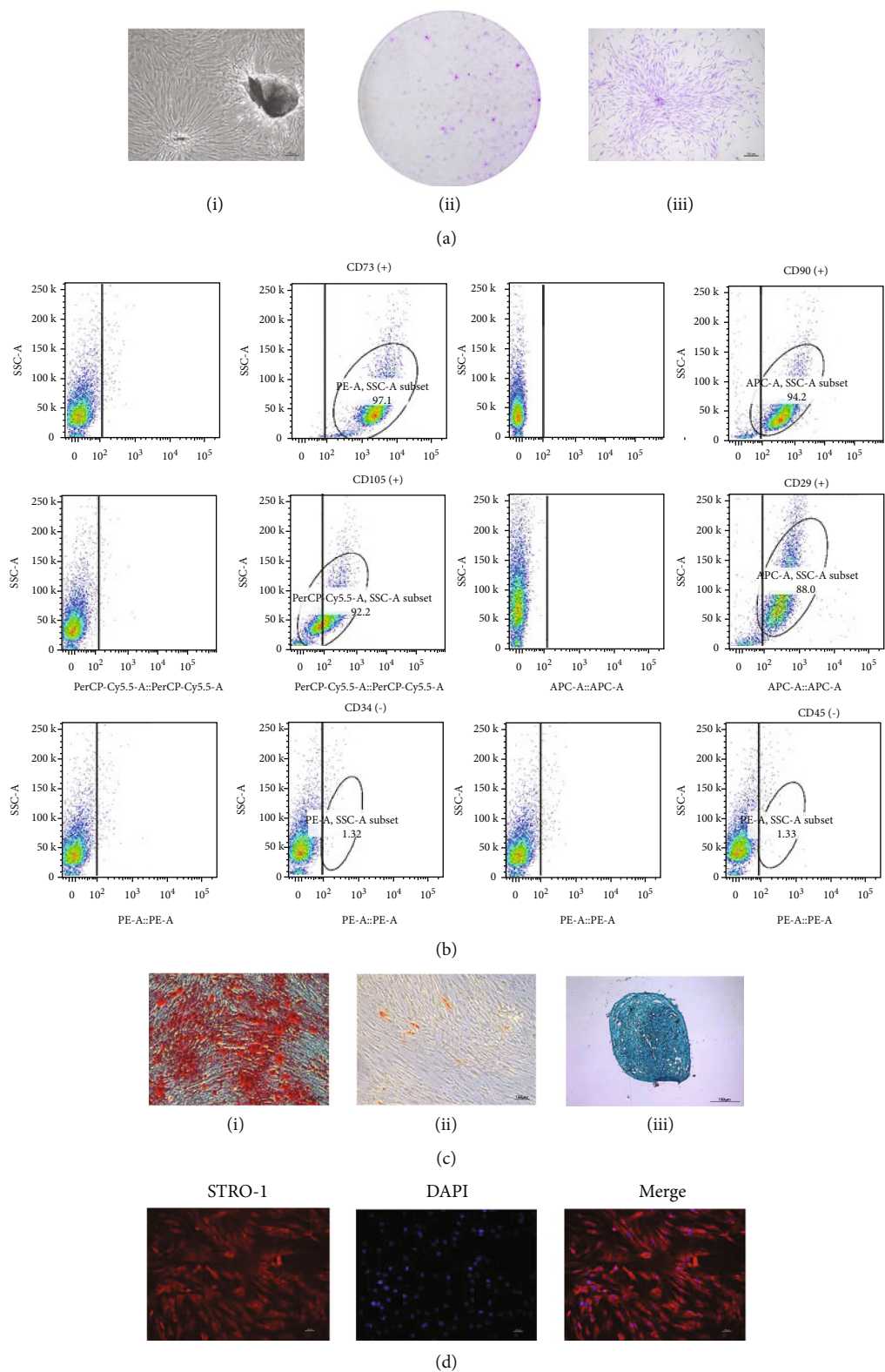


FIGURE 1: Identification of PDLSCs and verification of PDLSC multidirectional differentiation ability. (a): (I) Primary cells migrated from PDL tissues on day 3, and 80% confluence was observed on day 12 (scale bar: 100 μ m). (II, III) Cell colonies formed by PDLSCs observed in the dish and an amplified image of a representative colony captured by a microscope (scale bar: 100 μ m). (b) Flow cytometry results showed that CD29, CD73, CD90, and CD105 were positive in PDLSCs. In addition, both CD45 and CD34 were negative. (c) Multiple differentiation potentials of PDLSCs (from left to right: osteogenesis, adipogenesis, chondrogenesis; scale bar: 100 μ m). (d) Immunofluorescence assay revealed that cultured PDLSCs were positive for STRO-1 (scale bar: 100 μ m).

- (2) Characteristic staining was performed, respectively, to prove that PDLSCs had the ability of multidirectional differentiation into osteogenic, adipogenic, and chondrogenic (Figure 1(c)). Immunofluorescence results showed positive expression of STRO-1 (Figure 1(d)).

3.2. *circFAT1* Does Not Affect PDLSCs Proliferation

- (1) CCK8 assay verified that PDLSCs transfection of *circFAT1* siRNA had no significant effect on proliferation (Figure 2(a)). DNA replication ability of cells was detected by EdU assay, which further confirmed that the effect of *circFAT1* on the proliferation of PDLSCs is not significant (Figures 2(a) and 2(b)).
- (2) PCR gel electrophoresis verified that the primers were located at a single band of 449 kb. The cyclization site of *circFAT1* was determined by plasmid vector construction (Figure 2(c)). The results of RNA nucleocytoplasmic isolation proved that *circFAT1* was mostly distributed in the cytoplasm (Figure 2(d)).

3.3. *circFAT1* Silencing Inhibits Osteoblastic Differentiation Potential of PDLSCs. To detect whether *circFAT1* affects the osteogenic differentiation potential of PDLSCs, cells were transfected with NC or *circFAT1* siRNA (si-FAT1), respectively. Western blot and RT-qPCR showed that biomarkers of osteogenesis (RUNX2, OSX, COL1A, and COL3A) were downregulated, and RT-qPCR results showed that the *circFAT1* expression was decreased (Figures 3(a)–3(c)).

The osteogenic induction medium was used for culturing two groups of cells, respectively. ARS confirmed that the mineralization nodules in the si-FAT1 group were decreased, and the calcium content calculated by the CPC assay was significantly decreased ($P < 0.001$) on 14 days. ALP activity was detected after seven days, which was used as an indicator for early observation of the osteogenic differentiation ability of PDLSCs. We found that the si-FAT1 group expresses less ALP, and meanwhile, the activity of ALP decreased significantly ($P < 0.001$) (Figures 3(d) and 3(e)). Immunofluorescence experiments confirmed the reduced expression of ALP in the si-FAT1 group (Figure 3(f)).

3.4. *SMAD5* Regulates the Osteoblastic Differentiation Ability of PDLSCs. PDLSCs were transfected with NC or *SMAD5* siRNA (si-SMAD5). Western blot and RT-PCR results showed *SMAD5* and biomarkers of osteogenesis (RUNX2, OSX, COL1A, and COL3A) were downregulated (Figures 4(a)–4(c)).

The osteogenic induction medium was used for culturing two groups of cells, respectively. At 14 days, the CPC assay and ARS results showed that the mineralization nodules and calcium content in the si-SMAD5 group were significantly reduced ($P < 0.001$). After seven days, to early observe the osteogenic differentiation ability of PDLSCs, ALP activity was performed. The results proved that the expression of ALP in the si-SMAD5 group was reduced, and the ALP activity decreased significantly ($P < 0.001$) (Figures 4(d) and 4(e)). Immunofluorescence experiments

confirmed that the expression of ALP in PDLSCs in the si-SMAD5 group was significantly downregulated (Figure 4(f)).

3.5. Overexpression of *miR-4781-3p* Decreases Osteoblastic Differentiation Tendency of PDLSCs. PDLSCs were transfected with NC for mimics or *miR-4781-3p* mimics (mimics), respectively. Western blot and RT-qPCR showed that *SMAD5* and biomarkers of osteogenesis (RUNX2, OSX, COL1A, and COL3A) were reduced. In addition, RT-PCR results displayed less expression of *circFAT1* and increased expression of *miR-4781-3p* (Figures 5(a)–5(c)).

The mineralization induction medium was used for culturing two groups of PDLSCs, and ARS and CPC assay was performed at 14 days. It was found that the mineralization nodules and calcium content of the mimics group were significantly reduced ($P < 0.001$). After a week, the ALP activity was detected, less expression of ALP was found in the mimics group, and the ALP activity was downregulated significantly ($P < 0.001$) (Figures 5(d) and 5(e)). Immunofluorescence experiments confirmed that the expression of ALP in PDLSCs in the mimics group was significantly reduced (Figure 5(f)).

3.6. Knockdown of *miR-4781-3p* Increases Osteoblastic Differentiation Tendency of PDLSCs. PDLSCs were transfected with negative inhibitor control (iNC) or *miR-4781-3p* inhibitor (inhibitor), respectively. Western blot and RT-qPCR showed that the expression of *SMAD5* and biomarkers of osteogenesis (RUNX2, OSX, COL1A, and COL3A) increased. In addition, RT-qPCR results showed that the *circFAT1* expression was increased while the expression of *miR-4781-3p* was decreased (Figures 6(a)–6(c)).

The mineralization induction medium was used for culturing two groups of PDLSCs. ARS and CPC determination were performed on the 14th day. The results showed that mineralized nodules and calcium content increased significantly in the inhibitor group ($P < 0.001$). ALP activity was detected after a week, and the results showed that an increasing ALP expression in the inhibitor group and ALP activity was also upregulated ($P < 0.001$) (Figures 6(d) and 6(e)). Immunofluorescence analysis confirmed that the ALP expression was promoted in the inhibitor group (Figure 6(f)).

3.7. *circFAT1* Acting as a *miRNA* Sponge for *miR-4781-3p* by Targeting *SMAD5*. To verify the sponge effect of *circFAT1* as *miR-4781-3p* competitively combining *SMAD5*, *circFAT1* wild-type (FAT1 WT) and mutant plasmid (FAT1 MT) were constructed, respectively. By cotransfection with *miR-4781* negative control (NC) and *miR-4781* mimics (mimics), dual-luciferase reporter assay showed that *miR-4781* mimics significantly inhibited the luciferase activity of *circFAT1* wild-type reporter gene and confirm the existence of binding sites (Figure 7(a)). *SMAD5* wild-type (*SMAD5* WT) and mutant plasmid (*SMAD5* MT) were constructed, respectively. By cotransfection with *miR-4781* negative control (NC) and *miR-4781* mimics (mimics), dual-luciferase reporter assay showed that *miR-4781* mimics significantly inhibited the luciferase activity of *SMAD5* wild-type reporter

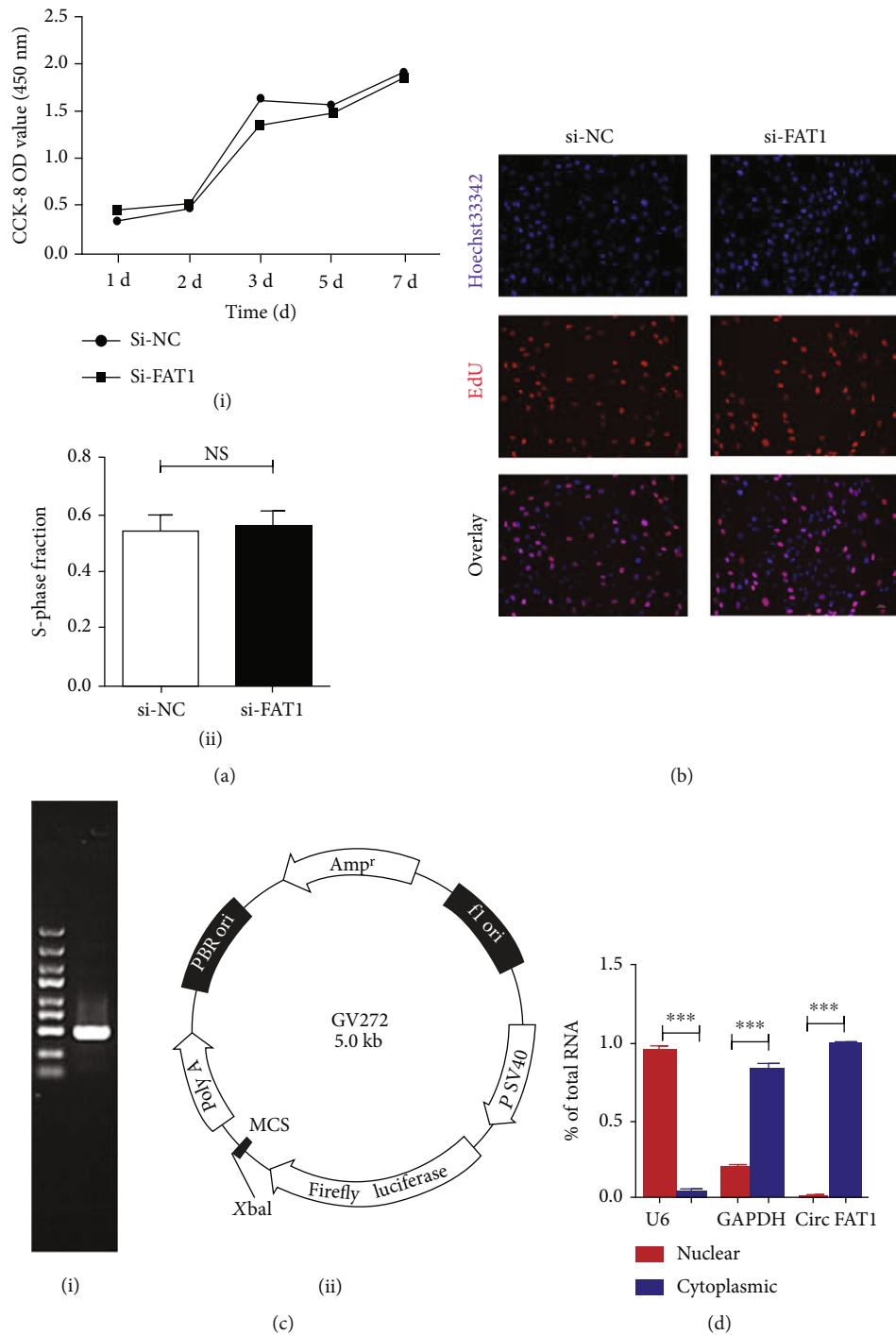


FIGURE 2: circFAT1 does not affect PDLSCs proliferation. (a) Cell proliferation capability influenced by circFAT1 was detected at 450 nm with CCK-8 assay. (I): CCK-8 results showed that circFAT1 had no significant effect on the proliferation of PDLSCs; (II): EdU assay further confirmed that circFAT1 had no significant effect on the proliferation of PDLSCs. (b) EdU-positive PDLSCs influenced by circFAT1 were detected by EdU kit (scale bar: 200 μ m). EdU (red), Hoechst333 (blue). (c) PCR gel electrophoresis verified that the primers were located at a single band of 449 kb. The cyclization site of circFAT1 was determined by plasmid vector construction. (d) RNA nucleocytoplasmic isolation experiments verified that circFAT1 was mainly located in the cytoplasm of cells. * $P < 0.05$, ** $P < 0.01$, and *** $P < 0.001$. EdU: 5-ethynyl-2-deoxyuridine.

gene and confirm the existence of binding sites between SMAD5 and miR-4781 (Figure 7(a)).

Meanwhile, a rescue experiment was carried out to further verify. The western blot results revealed that inhibit-

ing miR-4781 could reverse the inhibitory effect of circFAT1 siRNA on the osteogenic ability of PDLSCs. And the miR-4781 inhibitor reversed the expression of SMAD5 (Figure 7(b)).

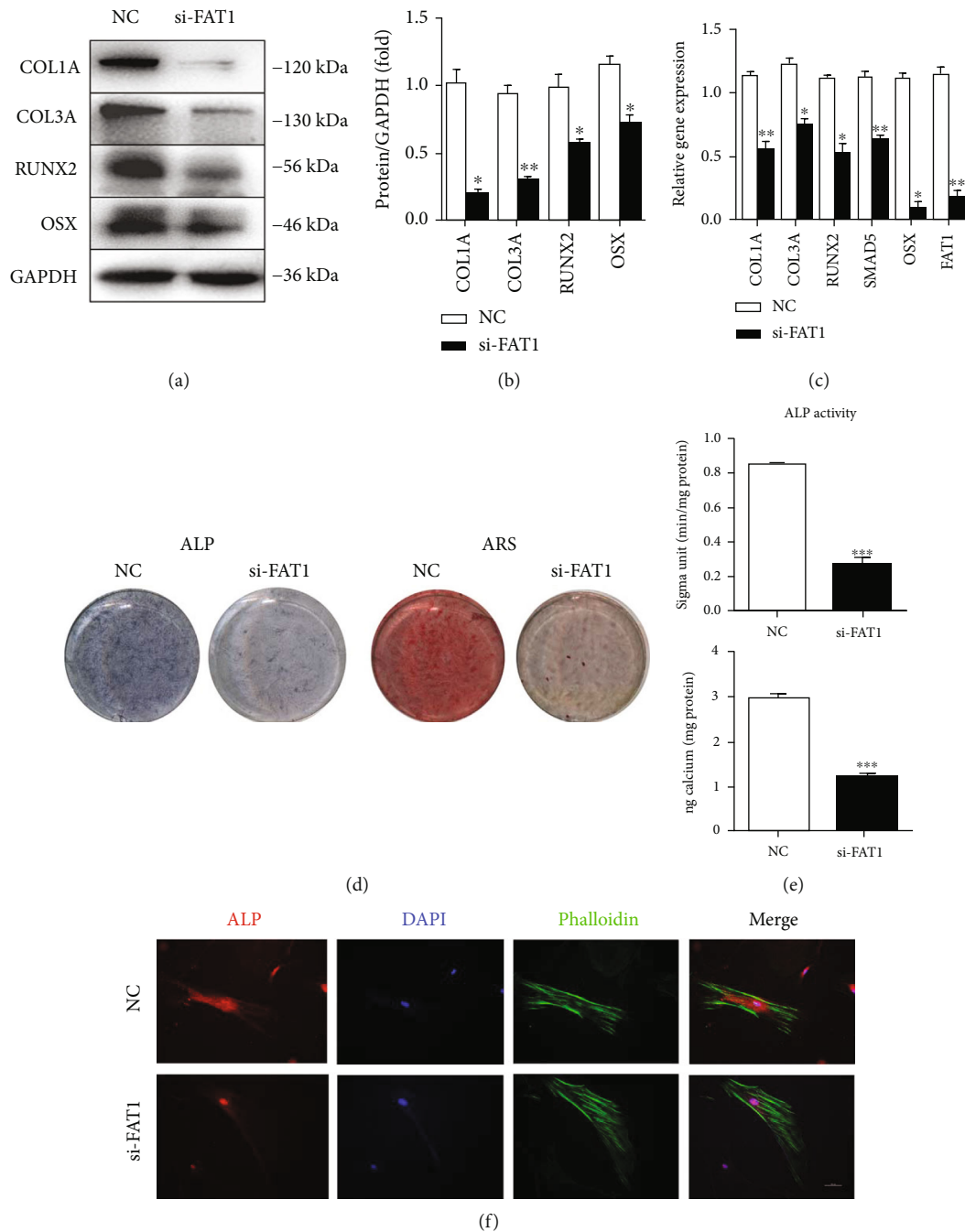


FIGURE 3: circFAT1 silencing inhibits osteoblastic differentiation potential of PDLSCs. (a)–(c) Western blot and RT-qPCR showed that osteogenic markers (RUNX2, OSX, COL1A, and COL3A) were downregulated in the circFAT1 siRNA-treated PDLSCs (si-FAT1 group). (d, e) Silence of circFAT1 reduced the ALP activity of PDLSCs 7 days after osteogenic induction. ARS showed the mineralization of PDLSCs was decreased significantly in the si-FAT1 group after osteogenic induction for 14 days. (f) Immunofluorescence experiments confirmed the decreased expression of ALP in the si-FAT1 group. * $P < 0.05$, ** $P < 0.01$, and *** $P < 0.001$.

The osteogenic induction medium was used for culturing four groups of cells, respectively. CPC assay and ARS were performed at 14 days, and it was found that the mineralization nodules in the si-FAT1 group and si-FAT1 + miR-4781 iNC group decreased. Mineralized nodules were significantly increased in the si-FAT1 + inhibitor group, and calcium content was significantly increased ($P < 0.001$).

After seven days, less expression of ALP was found in the si-FAT1 group and si-FAT1 + miR-4781 iNC group, while the expression of ALP increased in the si-FAT1 + inhibitor group. ALP activity showed the same trend (Figures 7(c) and 7(d)). FISH experiments proved that circFAT1 was mostly located in the cytoplasm, and 18S and U6 were detected as the internal control (Figure 7(e)).

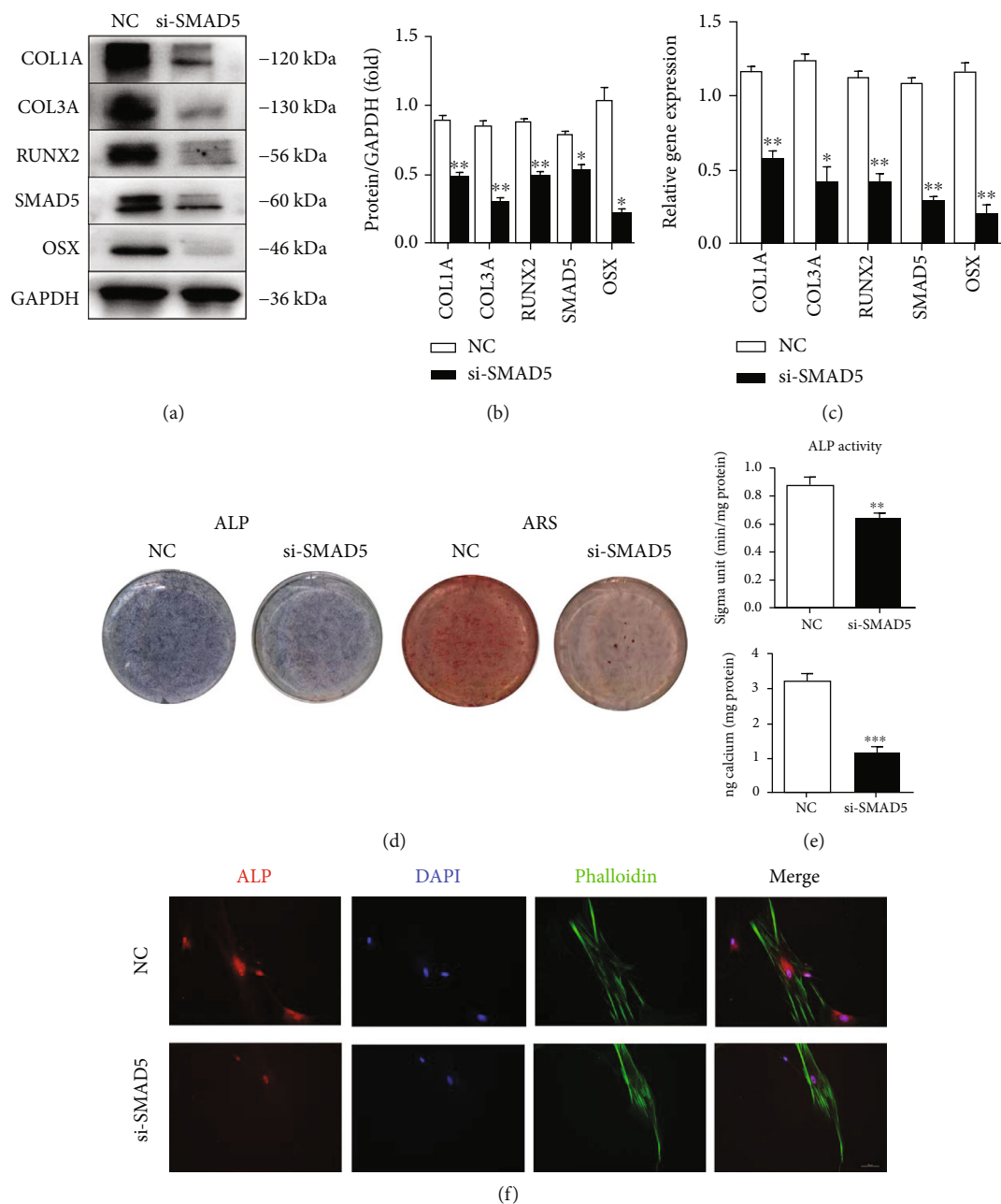


FIGURE 4: SMAD5 regulates the osteoblastic differentiation ability of PDLSCs. (a)–(c) Western blot and RT-qPCR showed that osteogenic markers (RUNX2, OSX, COL1A, and COL3A) were downregulated in the SMAD5 siRNA-treated PDLSCs (si-SMAD5 group). (d, e) Silence of SMAD5 reduced the ALP activity of PDLSCs 7 days after osteogenic induction. ARS showed the mineralization of PDLSCs was decreased significantly in the si-SMAD5 group after osteogenic induction for 14 days. (f) Immunofluorescence experiments confirmed the decreased expression of ALP in the si-SMAD5 group. * $P < 0.05$, ** $P < 0.01$, and *** $P < 0.001$.

3.8. Silence of circFAT1 Inhibits the Osteogenic Differentiation Ability of PDLSCs In Vivo. To further understand the role of circFAT1, the skull defect model of SD rats was constructed (Figure 8(a)). PDLSC cell mass transfected with NC or circFAT1 siRNA (si-FAT1) was placed, respectively, and the tissue samples were taken eight weeks later. 3D reconstruction image of the rat skull showed that bone regeneration in the si-FAT1 group was inhibited (Figure 8(b)). H&E and Masson

staining results indicated that the new bone mass in the si-FAT1 group was significantly reduced. The bone volume fraction was decreased in the si-FAT1 group by calculating the ratio of bone volume and tissue volume (BV/TV) ($P < 0.01$) (Figures 8(c) and 8(d)). Therefore, as shown in the pattern diagram, circFAT1 may regulate PDLSC osteoblastic regeneration by targeting SMAD5 through acting as a sponge for miR-4781-3p (Figure 8(e)).

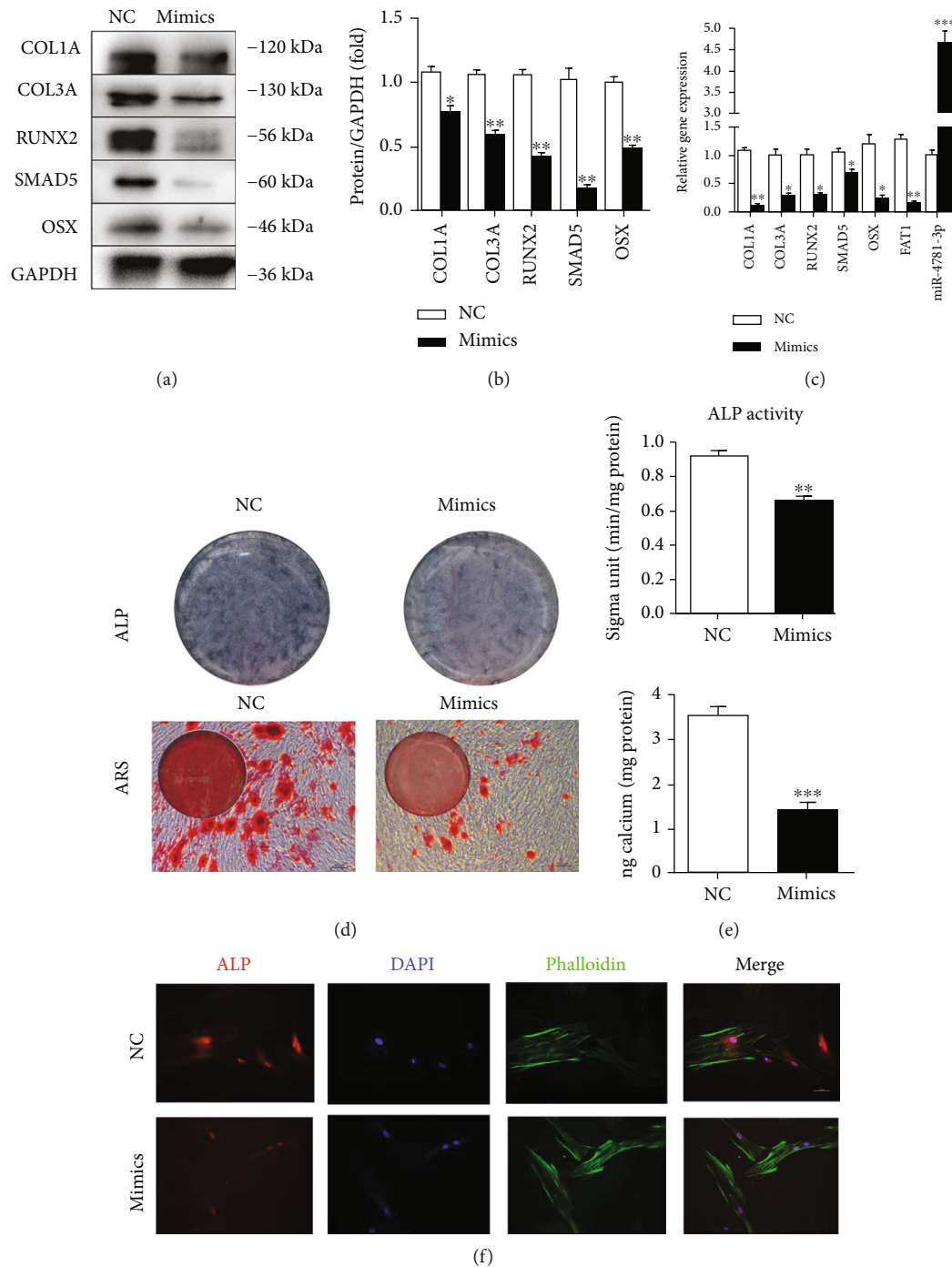


FIGURE 5: Overexpression of miR-4781-3p decreases osteoblastic differentiation tendency of PDLSCs. (a)–(c) The results of Western blot and RT-qPCR showed SMAD5 and osteogenic markers (RUNX2, OSX, COL1A, and COL3A) were downregulated in miR-4781-3p mimic transfected PDLSCs (mimics group). In addition, RT-qPCR results showed that the expression of *circFAT1* was downregulated, and *miR-4781-3p* was upregulated in the mimics group. (d, e) Overexpression of miR-4781-3p reduced the ALP activity of PDLSCs 7 days after osteogenic induction. ARS showed the mineralization of PDLSCs was decreased significantly in the mimic group after osteogenic induction for 14 days. (f) Immunofluorescence experiments confirmed the decreased expression of ALP in the mimics group. * $P < 0.05$, ** $P < 0.01$, and *** $P < 0.001$.

4. Discussion

As one of the most common oral inflammatory diseases, periodontitis is often related to human tooth loss. For peri-

odontal tissue with complex structure, tissue regeneration and stable microenvironment are challenging for currently available treatments. In regenerative therapy, since MSCs can be obtained from various tissues, stem cell therapy has

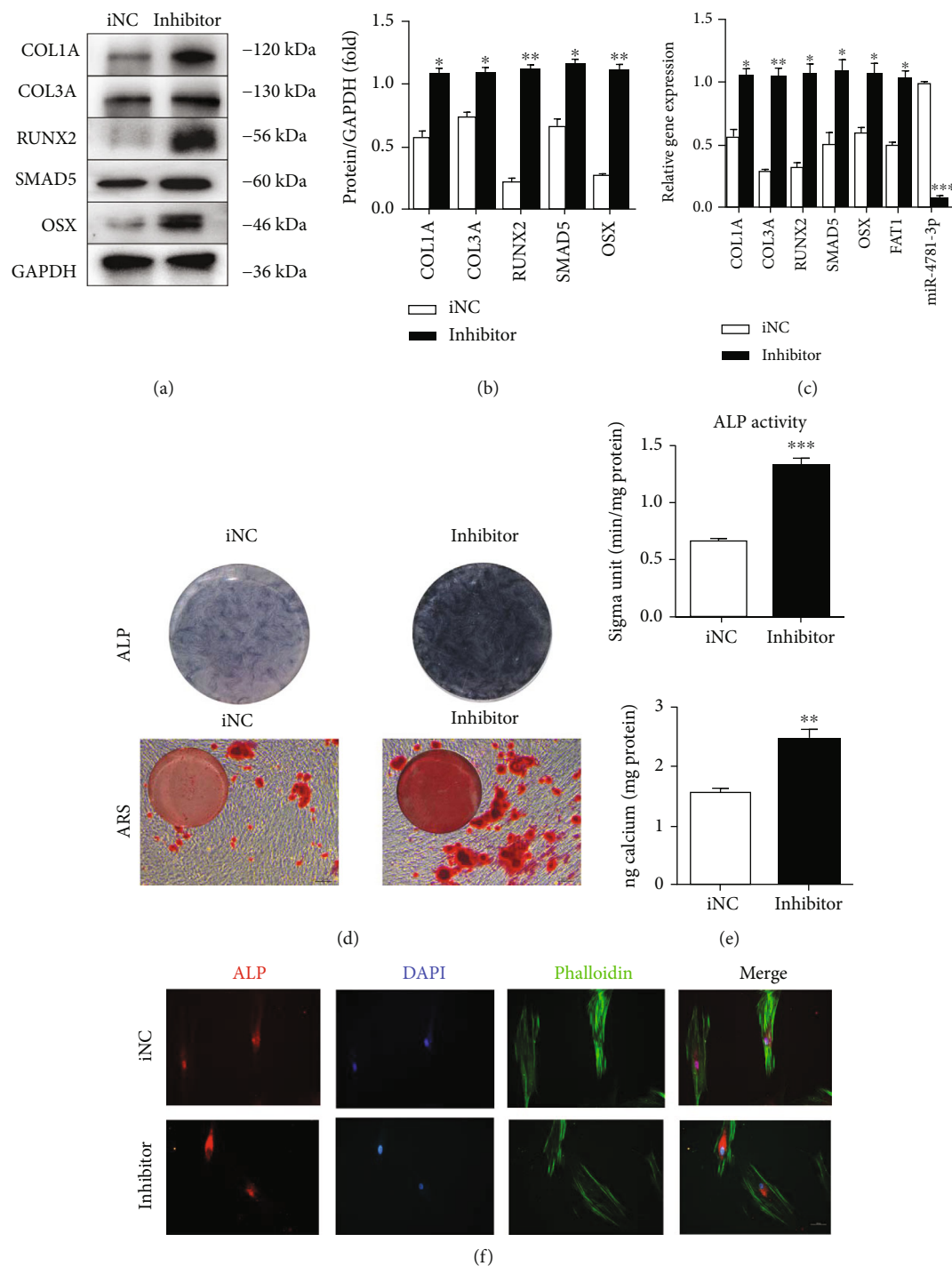


FIGURE 6: Knockdown of miR-4781-3p increases osteoblastic differentiation tendency of PDLSCs. (a)–(c) The results of Western blot and RT-qPCR showed SMAD5 and osteogenic markers (RUNX2, OSX, COL1A, and COL3A) were upregulated in the miR-4781-3p inhibitor transfected PDLSCs (inhibitor group). In addition, RT-qPCR results showed that the expression of *circFAT1* was upregulated, and *miR-4781-3p* was downregulated in the inhibitor group. (d, e) Knockdown of miR-4781-3p increased the ALP activity of PDLSCs 7 days after osteogenic induction. ARS showed the mineralization of PDLSCs was added significantly in the inhibitor group after osteogenic induction for 14 days. (f) Immunofluorescence experiments confirmed the increased expression of ALP in the inhibitor group. * $P < 0.05$, ** $P < 0.01$, and *** $P < 0.001$.

attracted more and more attention. PDLSCs are considered the best cell source for periodontal tissue regeneration [33]. In our previous study, LncNEAT1 may target miR-214-5p/

SMAD4 to regulate the cementogenic differentiation of PDLSCs (preprint) [34]. Seo et al. [35] found that PDLSCs can create a cementum/periodontal ligament-like structure

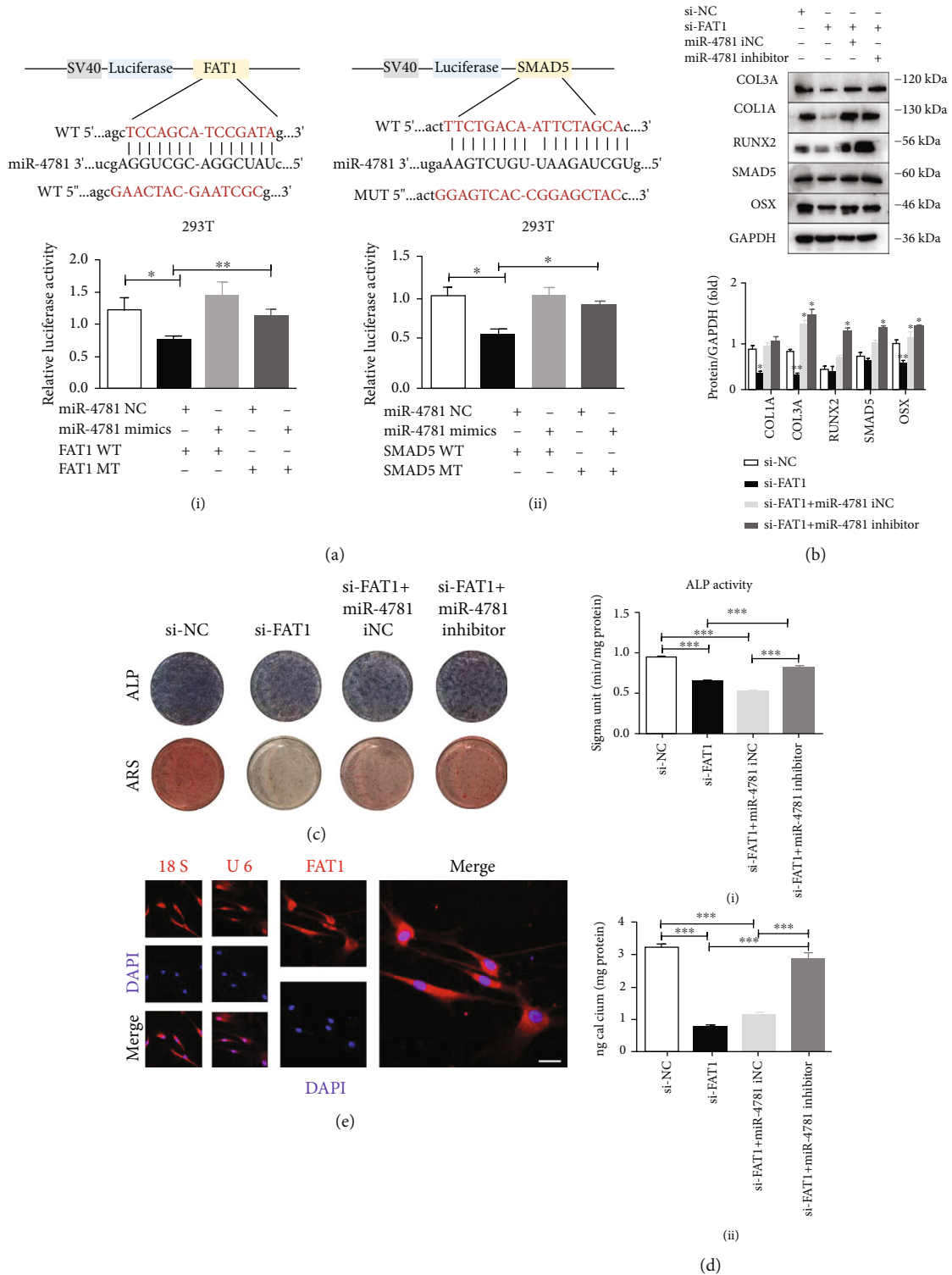


FIGURE 7: circFAT1 acting as a miRNA sponge for miR-4781-3p by targeting SMAD5. (a) I: Dual-luciferase reporter gene assay was used to verify the binding sites between circFAT1 and miR-4781-3p. II: Dual-luciferase reporter gene assay was used to verify the binding sites between SMAD5 and miR-4781-3p. (b) Rescue experiment results showed that miR-4781 inhibitor could reverse the inhibition of circFAT1 siRNA on the osteogenic ability of PDLSCs. The expression level of SMAD5 was also reversed by miR-4781 inhibitor. (c) After seven days, less expression of ALP was found in the si-FAT1 group and si-FAT1 + miR-4781 iNC group, while the expression of ALP increased in the si-FAT1 + inhibitor group. The mineralization nodules in the si-FAT1 group and si-FAT1 + miR-4781 iNC group decreased. (d) I: ALP activity showed the same trend. II: Mineralized nodules were significantly increased in the si-FAT1 + inhibitor group, and calcium content was significantly increased ($P < 0.001$). (e) FISH experiments proved that circFAT1 was mostly located in the cytoplasm, 18S and U6 were the internal control. (Scale bar: 25 μ m). * $P < 0.05$, ** $P < 0.01$, and *** $P < 0.001$.

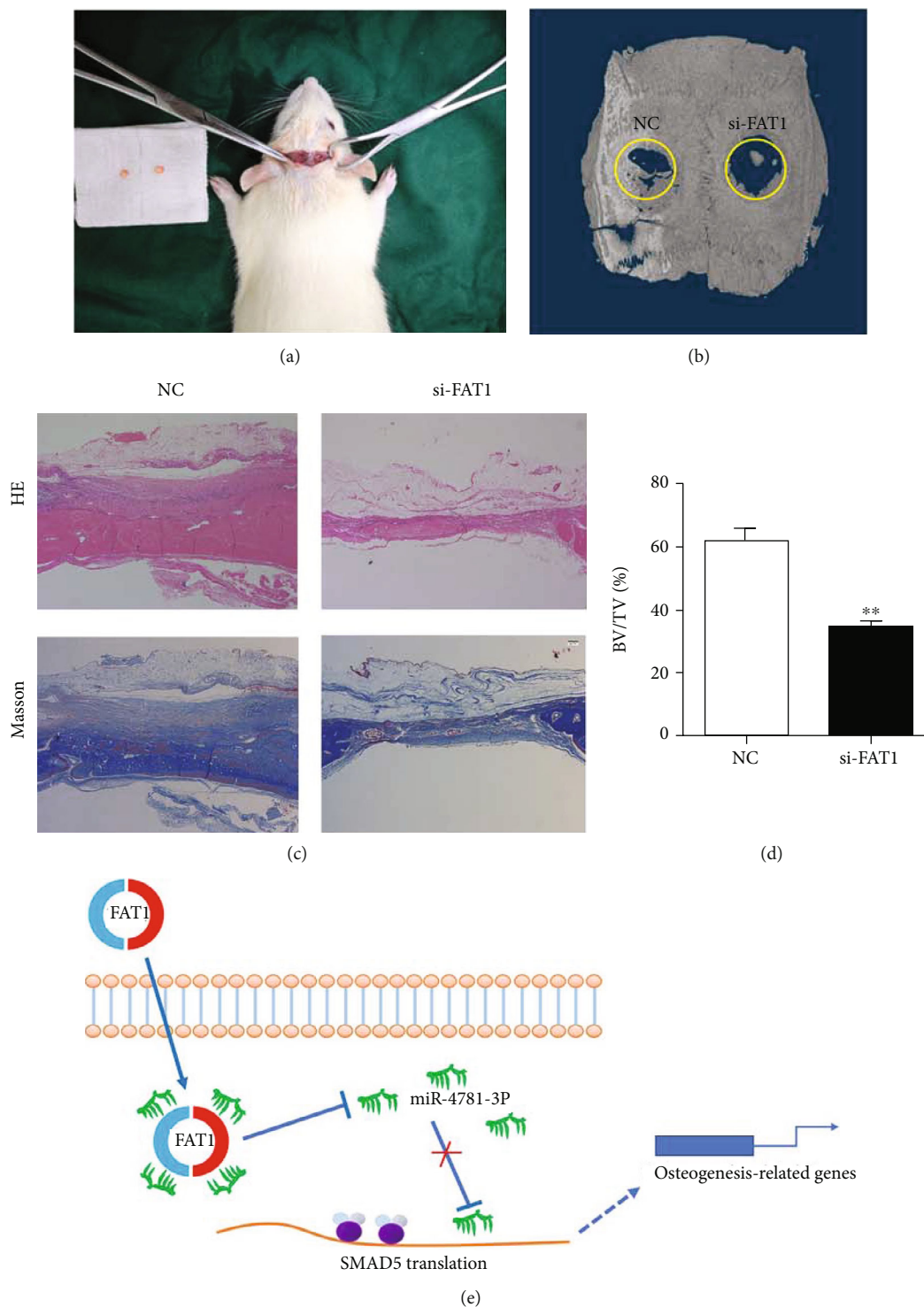


FIGURE 8: Silence of circFAT1 inhibits the osteogenic differentiation ability of PDLSCs in vivo. (a) The skull defect model of SD rats was constructed. (b) 3D reconstruction image of the rat skull showed that bone regeneration in si-FAT1 group was inhibited. (c) H&E staining and Masson staining results both indicated that the new bone mass in the si-FAT1 group was significantly reduced. (Scale bar: 50 μ m) (d) The bone volume fraction (BV/TV) was decreased in the si-FAT1 group. (e) Experimental mechanism diagram: circFAT1 may regulate PDLSC bone regeneration by targeting SMAD5 through acting as a sponge for miR-4781-3p. * $P < 0.05$, ** $P < 0.01$, and *** $P < 0.001$.

in vivo. Therefore, PDLSCs may be the key to periodontal tissue regeneration [35]. Although odontogenic stem cells can differentiate into various compartments, the number of cells that can perform the required functions is limited.

Therefore, it is vital to induce PDLSCs to differentiate into osteoblasts and cementoblasts [36].

SMAD5 is considered to be involved in regulating osteogenic differentiation [37]. After bone morphogenetic protein

2 (BMP-2) binds to the receptor in the bone morphogenetic protein (BMP) pathway, SMAD5 is activated by phosphorylation and binds to SMAD1 and SMAD8 to form polymers and then transferred to the nucleus and positively regulated the transcription of osteogenic genes [38]. This regulatory effect is mainly achieved by interacting with various transcription regulators, targeting several *cis*-acting promoter elements among osteogenic genes like ALP and osteocalcin (OCN). It is worth noting that the upregulation of RUNX2, as a SMAD5 transcription factor, largely determines this effect [39]. Many studies have confirmed that miRNAs targeting SMAD5 inhibit osteogenic differentiation. In this study, we demonstrated the direct regulatory effect of miR-4781-3p on SMAD5. After SMAD5 knockout, the osteogenic differentiation potential of PDLSCs was limited, and the overexpression of miR-4781-3p could reverse this effect.

Recent studies have shown that circRNAs participate in various biological processes such as miRNA sponges, protein binding regulation, and gene transcription and may regulate multiple diseases, including periodontitis. Both *in vitro* [29, 40, 41] and *in vivo* [42, 43] studies have confirmed that circRNAs are involved in regulating the osteogenic differentiation of PDLSCs. In the process of PDLSCs' osteoblastic induction and mechanical stimulation, specific circRNAs were detected upregulated or downregulated. circCDK8 was proved to impair the osteogenesis of PDLSCs under hypoxia [29]. It is found that circRNA function through the network relationship between circRNAs and miRNAs. CircRNA 3140 targets miR-21, and circRNA 436 may act as a sponge for miR-107 and miR-335 [41, 44]. CircMAP3K11 may promote the proliferation of PDLSCs and inhibit their apoptosis by acting as a sponge for miR-511-3p [42]. CircCDR1as acts as a sponge for miR-7 in PDLSC proliferation and differentiation, affecting ERK or MAPK signaling pathways [43]. In addition, circRNAs may also regulate bone formation by regulating extracellular matrix tissue and cell differentiation and affect the BMP signaling pathway, according to sequencing analysis of osteogenic induced PDLSCs. Gu et al. [44] found that 766 circRNAs were upregulated, and 690 were downregulated in PDLSCs 7 days after osteogenic induction. It is reasonable to believe that the competing endogenous RNA (ceRNA) network seems to be the main mechanism for circRNAs to perform functions during the osteogenesis of PDLSCs [44]. However, it is still necessary to better understand all the potential mechanisms that may regulate circRNAs. Some studies have found circFAT1 can act as a sponge for miR-30a-5p in competitive combination with REEP3, thus influencing the progression of HCC [45], but there is no relevant research on the biological characteristics of circFAT1 and its role in oral diseases. It is worth noting that there seems to be no common circRNAs among different oral cell types. For instance, circ0081572 was found in gingival tissue (not cells) and PDLSCs [39]. These results suggest that circRNAs may be cell-specific in periodontal tissue. Because some circRNAs can change cell behaviors, it is promising to study it as a therapeutic target to regulate stem cell differentiation and optimize periodontal regeneration. Further research on cir-

crNAs is needed to understand their role in periodontal diagnosis and regeneration.

5. Conclusions

In this study, SMAD5 was found positively regulated the osteogenic differentiation of PDLSCs. miR-4781-3p may participate in inhibiting the protein translation of SMAD5, blocking its expression, and then reducing osteogenic differentiation of PDLSCs. The binding sites between SMAD5 and miR-4781-3p and between circFAT1 and miR-4781-3p were confirmed by analysis of dual-luciferase reporter assay, respectively. The functional relationship between the three was verified by rescue experiments. *In vivo*, inhibiting the expression of circFAT1 reduced the bone regeneration of rat skull defect. Therefore, combined with *in vivo* and *in vitro* studies, we could conclude that circFAT1 may be involved in the regulation of PDLSCs' osteogenic differentiation through the ceRNA network of miR-4781-3p/SMAD5. Whether there are other regulatory mechanisms remains to be further explored. Our research may be helpful to explore the role of circFAT1 in periodontal regeneration and verify the mechanism of its possible regulation of SMAD5 through sponging with miR-4781-3p, aiming to investigate the potential target of PDLSCs mediated periodontal bone regeneration.

Data Availability

The raw data used to support the findings of this study are available from the corresponding author upon request.

Conflicts of Interest

The authors declare that they have no competing interests.

Acknowledgments

This work was supported by the National Natural Science Foundation of China (grant numbers: 81873707, 82170940, and 81900962).

References

- [1] P. Monsarrat, J. N. Vergnes, C. Nabet et al., "Concise review: mesenchymal stromal cells used for periodontal regeneration: a systematic review," *Stem Cells Translational Medicine*, vol. 3, no. 6, pp. 768–774, 2014.
- [2] L. Qi and Y. Zhang, "The microRNA 132 regulates fluid shear stress-induced differentiation in periodontal ligament cells through mTOR signaling pathway," *Cellular Physiology and Biochemistry*, vol. 33, no. 2, pp. 433–445, 2014.
- [3] J. C. Lim and C. H. Mitchell, "Inflammation, pain, and pressure-purinergic signaling in oral tissues," *Journal of Dental Research*, vol. 91, no. 12, pp. 1103–1109, 2012.
- [4] Y. Yang, W. Yujiao, W. Fang et al., "The roles of miRNA, lncRNA and circRNA in the development of osteoporosis," *Biological Research*, vol. 53, no. 1, p. 40, 2020.

- [5] Y. Li, J. Li, L. Chen, and L. Xu, "The roles of long non-coding RNA in osteoporosis," *Current Stem Cell Research & Therapy*, vol. 15, no. 7, pp. 639–645, 2020.
- [6] J. G. Letarouilly, O. Broux, and A. Clabaut, "New insights into the epigenetics of osteoporosis," *Genomics*, vol. 111, no. 4, pp. 793–798, 2019.
- [7] Z. Chen and H. L. Liu, "Restoration of miR-1305 relieves the inhibitory effect of nicotine on periodontal ligament-derived stem cell proliferation, migration, and osteogenic differentiation," *Journal of Oral Pathology & Medicine*, vol. 46, no. 4, pp. 313–320, 2017.
- [8] S. Y. Jiang, D. Xue, Y. F. Xie et al., "The negative feedback regulation of microRNA-146a in human periodontal ligament cells after *Porphyromonas gingivalis* lipopolysaccharide stimulation," *Inflammation Research*, vol. 64, no. 6, pp. 441–451, 2015.
- [9] F. Wei, D. Liu, C. Feng et al., "microRNA-21 mediates stretch-induced osteogenic differentiation in human periodontal ligament stem cells," *Stem Cells and Development*, vol. 24, no. 3, pp. 312–319, 2015.
- [10] K. Miyazono, Y. Kamiya, and M. Morikawa, "Bone morphogenetic protein receptors and signal transduction," *Journal of Biochemistry*, vol. 147, no. 1, pp. 35–51, 2010.
- [11] J. Yan, D. Guo, S. Yang, H. Sun, B. Wu, and D. Zhou, "Inhibition of miR-222-3p activity promoted osteogenic differentiation of hBMSCs by regulating Smad5-RUNX2 signal axis," *Biochemical and Biophysical Research Communications*, vol. 470, no. 3, pp. 498–503, 2016.
- [12] W. Zhang, L. Chen, J. Wu et al., "Long noncoding RNA TUG1 inhibits osteogenesis of bone marrow mesenchymal stem cells via Smad5 after irradiation," *Theranostics*, vol. 9, no. 8, pp. 2198–2208, 2019.
- [13] Z. Li, Y. Sun, S. Cao, J. Zhang, and J. Wei, "Downregulation of miR-24-3p promotes osteogenic differentiation of human periodontal ligament stem cells by targeting SMAD family member 5," *Journal of Cellular Physiology*, vol. 234, no. 5, pp. 7411–7419, 2019.
- [14] T. Fang, Q. Wu, L. Zhou, S. Mu, and Q. Fu, "miR-106b-5p and miR-17-5p suppress osteogenic differentiation by targeting Smad5 and inhibit bone formation," *Experimental Cell Research*, vol. 347, no. 1, pp. 74–82, 2016.
- [15] F. Wei, S. Yang, Q. Guo et al., "MicroRNA-21 regulates osteogenic differentiation of periodontal ligament stem cells by targeting Smad5," *Scientific Reports*, vol. 7, no. 1, p. 16608, 2017.
- [16] L. L. Chen and L. Yang, "Regulation of circRNA biogenesis," *RNA Biology*, vol. 12, no. 4, pp. 381–388, 2015.
- [17] S. Yang and X. Duan, "Epigenetics, Bone Remodeling and Osteoporosis," *Current stem cell research & therapy*, vol. 13, no. 2, 2018.
- [18] S. Qu, X. Yang, X. Li et al., "Circular RNA: a new star of non-coding RNAs," *Cancer Letters*, vol. 365, no. 2, pp. 141–148, 2015.
- [19] D. Rong, H. Sun, Z. Li et al., "An emerging function of circRNA-miRNAs-mRNA axis in human diseases," *Oncotarget*, vol. 8, no. 42, pp. 73271–73281, 2017.
- [20] S. Xu, L. Zhou, M. Ponnusamy et al., "A comprehensive review of circRNA: from purification and identification to disease marker potential," *PeerJ*, vol. 6, p. e5503, 2018.
- [21] S. Zhu, Y. Zhu, Z. Wang et al., "Bioinformatics analysis and identification of circular RNAs promoting the osteogenic differentiation of human bone marrow mesenchymal stem cells on titanium treated by surface mechanical attrition," *PeerJ*, vol. 8, article e9292, 2020.
- [22] C. Y. Yu, T. C. Li, Y. Y. Wu et al., "The circular RNA *circBIRC6* participates in the molecular circuitry controlling human pluripotency," *Nature Communications*, vol. 8, no. 1, p. 1149, 2017.
- [23] P. Zhu, X. Zhu, J. Wu et al., "IL-13 secreted by ILC2s promotes the self-renewal of intestinal stem cells through circular RNA *circPan3*," *Nature Immunology*, vol. 20, no. 2, pp. 183–194, 2019.
- [24] D. Y. Qian, G. B. Yan, B. Bai et al., "Differential circRNA expression profiles during the BMP2-induced osteogenic differentiation of MC3T3-E1 cells," *Biomedicine & Pharmacotherapy*, vol. 90, pp. 492–499, 2017.
- [25] C. Dou, Z. Cao, B. Yang et al., "Changing expression profiles of lncRNAs, mRNAs, circRNAs and miRNAs during osteoclastogenesis," *Scientific Reports*, vol. 6, no. 1, 2016.
- [26] L. Li, J. Guo, Y. Chen, C. Chang, and C. Xu, "Comprehensive CircRNA expression profile and selection of key CircRNAs during priming phase of rat liver regeneration," *BMC Genomics*, vol. 18, no. 1, p. 80, 2017.
- [27] T. B. Hansen, T. I. Jensen, B. H. Clausen et al., "Natural RNA circles function as efficient microRNA sponges," *Nature*, vol. 495, no. 7441, pp. 384–388, 2013.
- [28] X. Gu, X. Li, Y. Jin et al., "CDR1as regulated by hnRNPM maintains stemness of periodontal ligament stem cells via miR-7/KLF4," *Journal of Cellular and Molecular Medicine*, vol. 25, no. 9, pp. 4501–4515, 2021.
- [29] J. Zheng, X. Zhu, Y. He et al., "CircCDK8 regulates osteogenic differentiation and apoptosis of PDLSCs by inducing ER stress/autophagy during hypoxia," *Annals of the New York Academy of Sciences*, vol. 1485, no. 1, pp. 56–70, 2021.
- [30] W. Wu, J. Zhou, Y. Wu, X. Tang, and W. Zhu, "Overexpression of circRNA *circFAT1* in endometrial cancer cells increases their stemness by upregulating miR-21 through methylation," *Cancer Biotherapy & Radiopharmaceuticals*, 2021.
- [31] Y. Yao, X. Li, L. Cheng, X. Wu, and B. Wu, "Circular RNA FAT atypical cadherin 1 (*circFAT1*)/microRNA-525-5p/spindle and kinetochore-associated complex subunit 1 (*SKA1*) axis regulates oxaliplatin resistance in breast cancer by activating the notch and Wnt signaling pathway," *Bioengineered*, vol. 12, no. 1, pp. 4032–4043, 2021.
- [32] J. Satoh, Y. Kino, and S. Niida, "MicroRNA-Seq data analysis pipeline to identify blood biomarkers for Alzheimer's disease from public data," *Biomarker Insights*, vol. 10, pp. 21–31, 2015.
- [33] A. Queiroz, E. Albuquerque-Souza, L. M. Gasparoni et al., "Therapeutic potential of periodontal ligament stem cells," *World Journal of Stem Cells*, vol. 13, no. 6, pp. 605–618, 2021.
- [34] B. M. Seo, M. Miura, S. Gronthos et al., "Investigation of multipotent postnatal stem cells from human periodontal ligament," *Lancet*, vol. 364, no. 9429, pp. 149–155, 2004.
- [35] Y. Han, "High concentrations of calcium suppress osteogenic differentiation of human periodontal ligament stem cells in vitro," *Journal of Dental Sciences*, vol. 16, no. 3, pp. 817–824, 2021.
- [36] J. Dai, Y. Li, H. Zhou, J. Chen, M. Chen, and Z. Xiao, "Genistein promotion of osteogenic differentiation through BMP2/SMAD5/RUNX2 signaling," *International Journal of Biological Sciences*, vol. 9, no. 10, pp. 1089–1098, 2013.
- [37] Y. Gu, L. Ma, L. Song, X. Li, D. Chen, and X. Bai, "miR-155 inhibits mouse osteoblast differentiation by suppressing

- SMAD5 expression,” *BioMed research international*, vol. 2017, Article ID 1893520, 7 pages, 2017.
- [38] Y. Ito and K. Miyazono, “RUNX transcription factors as key targets of TGF- β superfamily signaling,” *Current Opinion in Genetics & Development*, vol. 13, no. 1, pp. 43–47, 2003.
- [39] J. Wang, C. Du, and L. Xu, “Circ_0081572 inhibits the progression of periodontitis through regulating the miR-378h/RORA axis,” *Archives of Oral Biology*, vol. 124, article 105053, 2021.
- [40] L. Xie, J. Chen, X. Ren et al., “Alteration of circRNA and lncRNA expression profile in exosomes derived from periodontal ligament stem cells undergoing osteogenic differentiation,” *Archives of Oral Biology*, vol. 121, article 104984, 2021.
- [41] B. Yu, J. Hu, Q. Li, and F. Wang, “CircMAP3K11 contributes to proliferation, apoptosis and migration of human periodontal ligament stem cells in inflammatory microenvironment by regulating TLR4 via miR-511 sponging,” *Frontiers in Pharmacology*, vol. 12, article 633353, 2021.
- [42] X. Li, Y. Zheng, Y. Zheng et al., “Circular RNA CDR1as regulates osteoblastic differentiation of periodontal ligament stem cells via the miR-7/GDF5/SMAD and p38 MAPK signaling pathway,” *Stem Cell Research & Therapy*, vol. 9, no. 1, p. 232, 2018.
- [43] H. Wang, C. Feng, Y. Jin, W. Tan, and F. Wei, “Identification and characterization of circular RNAs involved in mechanical force-induced periodontal ligament stem cells,” *Journal of Cellular Physiology*, vol. 234, no. 7, pp. 10166–10177, 2019.
- [44] X. Gu, M. Li, Y. Jin, D. Liu, and F. Wei, “Identification and integrated analysis of differentially expressed lncRNAs and circRNAs reveal the potential ceRNA networks during PDLSC osteogenic differentiation,” *BMC Genetics*, vol. 18, no. 1, p. 100, 2017.
- [45] H. Wei, S. Yan, Y. Hui et al., “CircFAT1 promotes hepatocellular carcinoma progression via miR-30a-5p/REEP3 pathway,” *Journal of Cellular and Molecular Medicine*, vol. 24, no. 24, pp. 14561–14570, 2020.